Supplementary Information

# Hybridizing amorphous $NiO_x$ nanoflakes and Mn-doped $Ni_2P$ nanosheet arrays for enhanced overall water electrocatalysis

Wen-Zhuo Zhang,[a,§] Guang-Yi Chen,[a,*,§] Jian Zhao,[*,a] Ji-Cai Liang,[a,b] Guang-Fei Liu,[a] Bao-Wei Ji[a] and Li-Feng Sun[a]

[a] School of Automotive Engineering, State Key Laboratory of Structural Analysis for Industrial Equipment, Dalian University of Technology, Dalian, 116024, China.

[b] Key Laboratory of Automobile Materials, Ministry of Education, and College of Materials Science and Engineering, Jilin University, Changchun, 130025, China.

* Correspondence author: E-mail: chengy@dlut.edu.cn (G. Y. Chen)

jzhao@dlut.edu.cn (J. Zhao)

§ Wen-zhuo Zhang and Guang-yi Chen contributed equally to this work

**Supporting Figures**

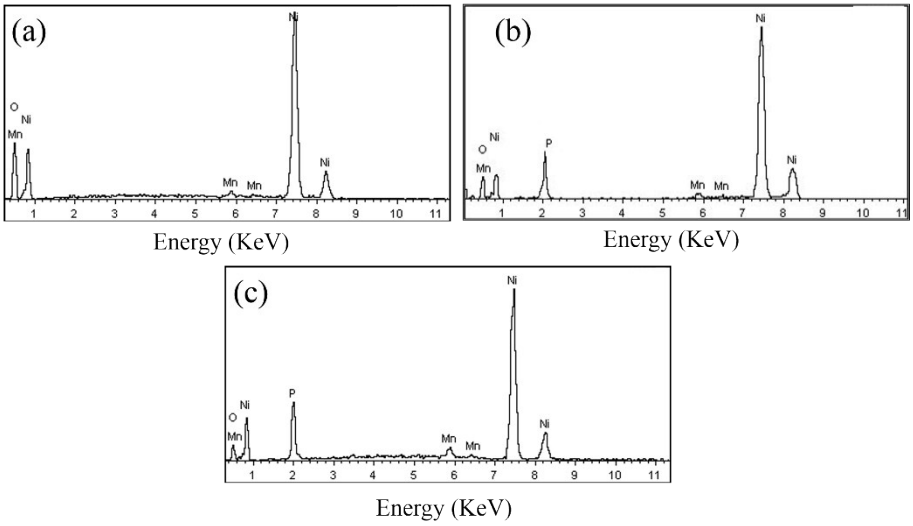


**Figure S1.** EDS spectrums of (a) $Mn_3$-$Ni_2P$, (b) $Mn_5$-$Ni_2P$ and (c) $Mn_7$-$Ni_2P$.

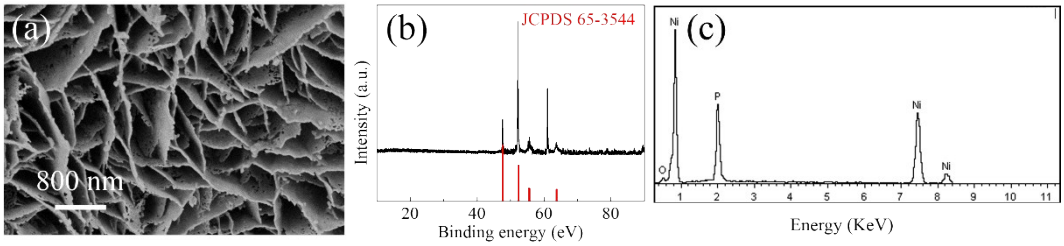


**Figure S2.** (a) SEM, (b) XRD and (c) EDS result of pure $Ni_2P$.

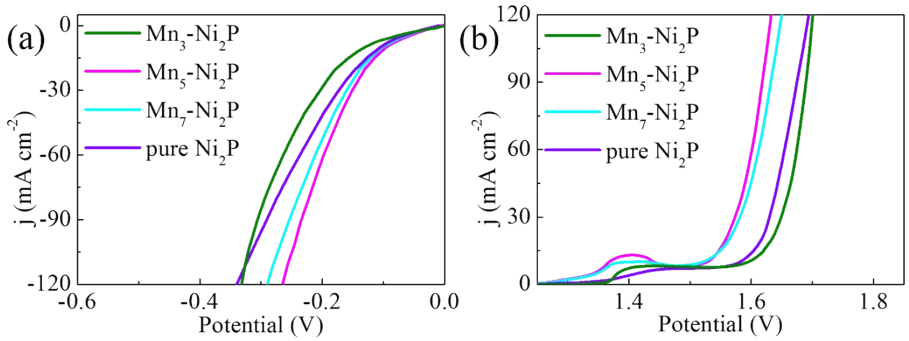


**Figure S3.** LSV curves of $Mn_x$-$Ni_2P$ and pure $Ni_2P$ for (a) HER and (b) OER.

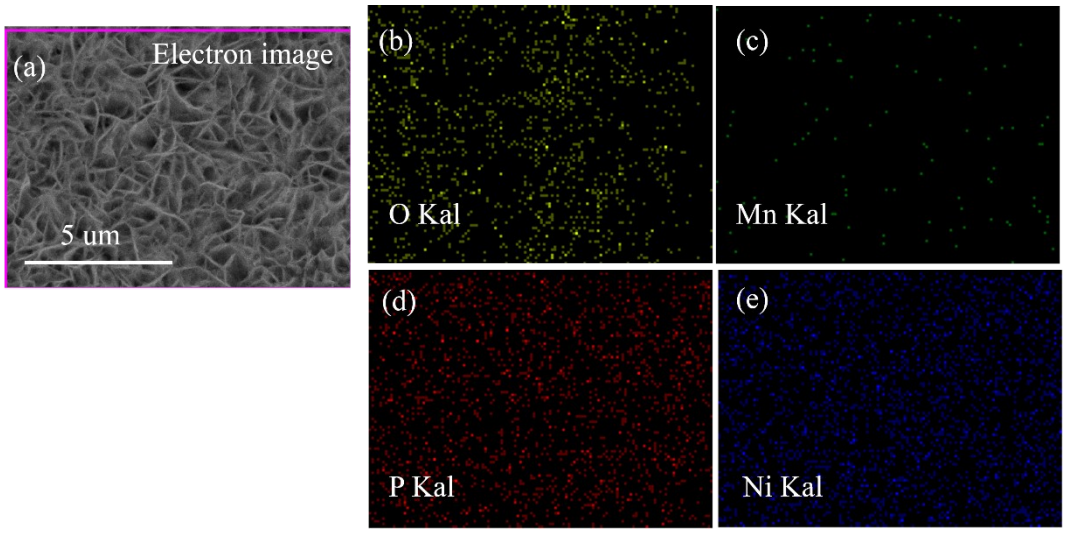


**Figure S4.** (a) Electron image of A-$NiO_x$-20/$Mn_5$-$Ni_2P$ and corresponding elemental mapping images of (b) O, (c) Mn, (d) P, and (e) Ni.

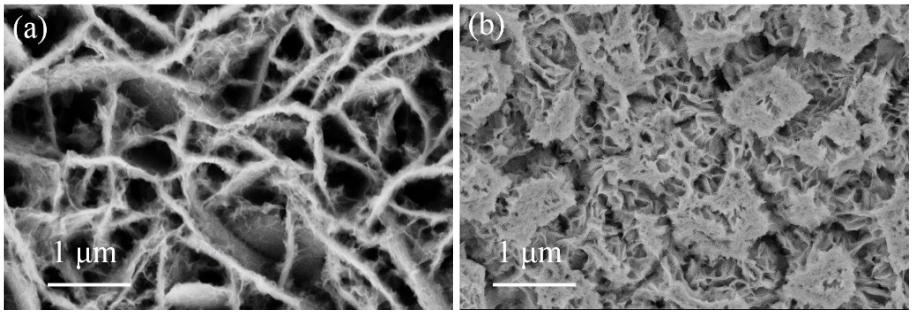


**Figure S5.** SEM images of (a) A-$NiO_x$-10/$Mn_5$-$Ni_2P$ and (b) A-$NiO_x$-30/$Mn_5$-$Ni_2P$.

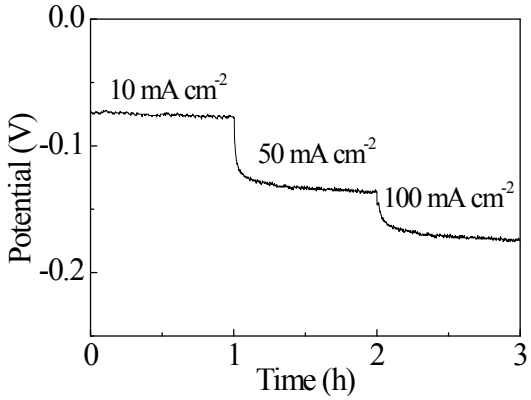


**Figure S6.** Controlled-current electrolysis of A-$NiO_x$-20/$Mn_5$-$Ni_2P$ at 10, 50 and 100 mA $cm^{-2}$ for HER.

**Table S1.** Comparison of the HER activity for several recently reported catalysts in 1 M KOH.

| Catalyst | Mass loading (mg $cm^{-2}$) | $\eta_{10}$ (mV) | Tafel (mV $dec^{-1}$) | Reference |
|---|---|---|---|---|
| A-$NiO_x$-20/$Mn_5$-$Ni_2P$ | 3.6 | 55 | 37 | This work |
| $Ni_8P_3$nanoflacs/NF | 10.58 | 130 | 58.5 | 1 |
| $Ni_xP$ nanosheets/CC | 25.8 | 117 | 85.4 | 2 |
| Am $FePO_4$/NF | 0.285 | 123 | 104.49 | 3 |
| Fe- and O-doping CoP nanowires/NF | 2.187 | 88 | 38.1 | 4 |
| CoP mesoporous nanorod /NF | 6.2 | 54 | 51 | 5 |
| CoNiP film | / | 82 | 43 | 6 |
| hierarchically structured NiCoP | 4.75 | 30 | 41 | 7 |
| CoP@$Ni_5P_4$@CoP/NF | / | 71 | 58 | 8 |
| CoP@Amorphous- $CoO_x$ /CC | 3 | 132 | 89 | 9 |
| CoP nanocrystal/Ti | 0.18 | 170 | 66 | 10 |
| $FeP_2$ nanowires/SS | 45 | 189 | 67 | 11 |
| NiS@$Ni_2P_2S_6$/NF | 1 | 140 | 72 | 12 |
| P-$Co_3O_4$/Ti | 0.4 | 120 | 52 | 13 |

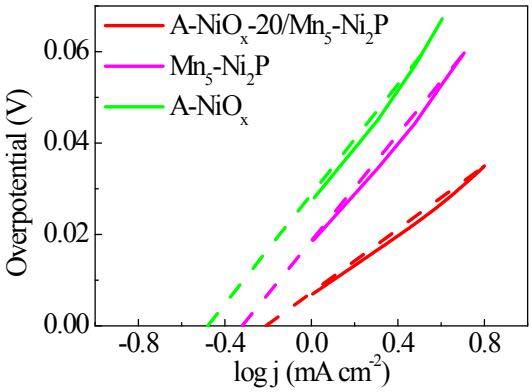


**Figure S7.** Calculated exchange current density of A-NiO$_x$-20/Mn$_5$-Ni$_2$P, Mn$_5$-Ni$_2$P and A-NiO$_x$ by using extrapolation methods.

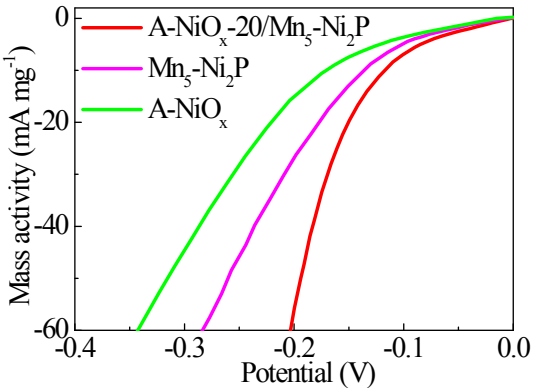


**Figure S8.** Mass activity of A-NiO$_x$-20/Mn$_5$-Ni$_2$P, Mn$_5$-Ni$_2$P and A-NiO$_x$ for HER.

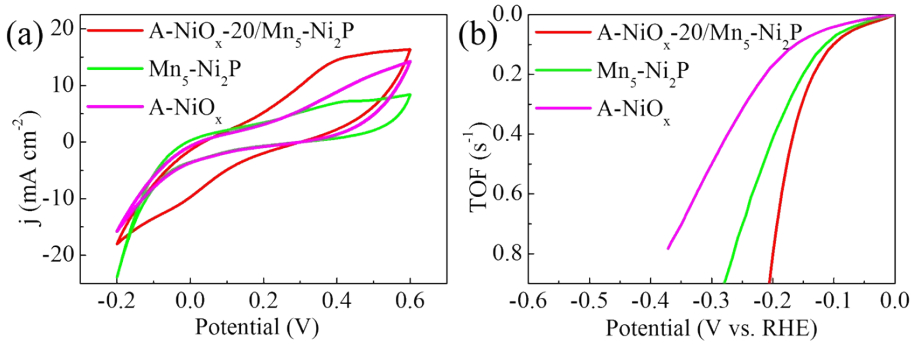


**Figure S9.** (a) CV curves of A-NiO$_x$-20/Mn$_5$-Ni$_2$P, Mn$_5$-Ni$_2$P and A-NiO$_x$ in 1 M PBS (pH=7) with a scan rate of 50mV/s. (b) Calculated TOF values of A-NiO$_x$-20/Mn$_5$-Ni$_2$P, Mn$_5$-Ni$_2$P and A-NiO$_x$ for HER.

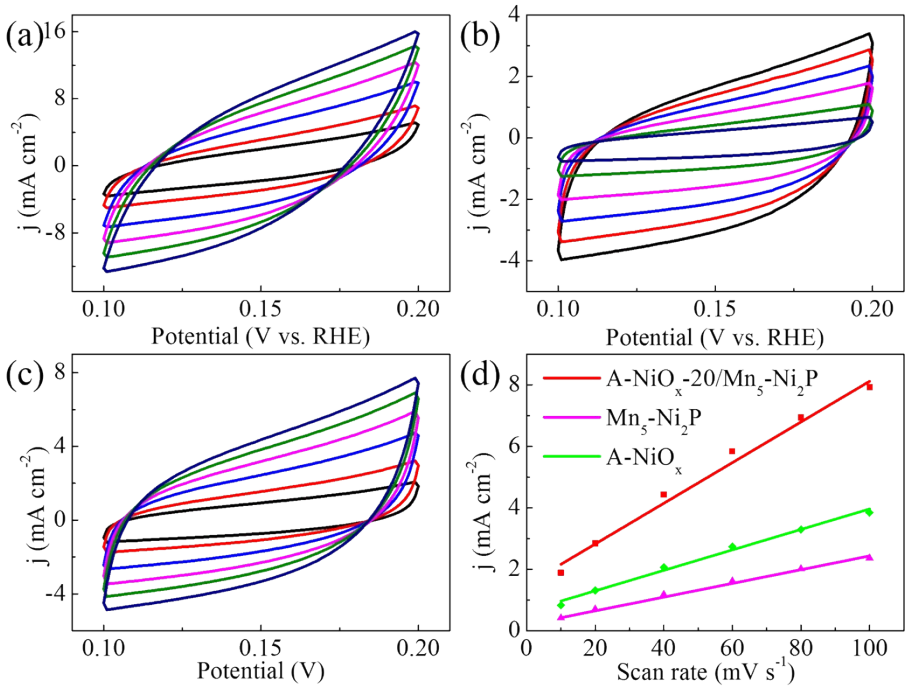


**Figure S10.** HER cyclic voltammograms for (a) A-$NiO_x$-20/$Mn_5$-$Ni_2P$, (b) $Mn_5$-$Ni_2P$ and (c) A-$NiO_x$ in the non-Faradaic capacitance current range from 0.1 to 0.2 V vs. RHE at scan rates of 10 (black curve), 20 (red curve), 40 (blue curve), 60 (magenta curve), 80 (olive curve), and 100 (navy curve) mV $s^{-1}$. (d) Scan rate dependence of the current densities of A-$NiO_x$-20/$Mn_5$-$Ni_2P$, $Mn_5$-$Ni_2P$ and A-$NiO_x$ at 0.15 V *vs.* RHE.

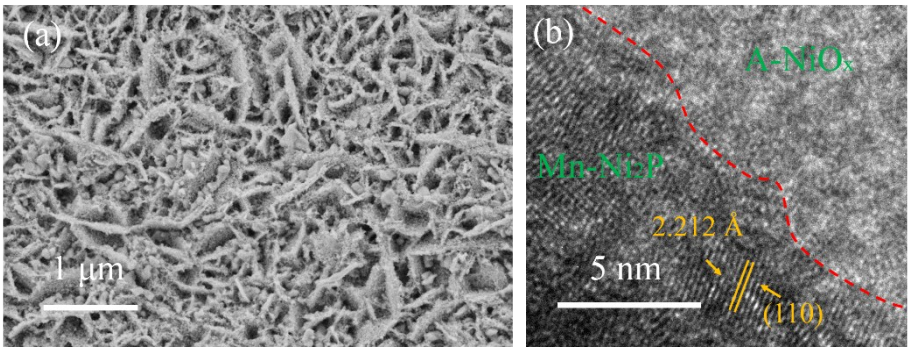


**Figure S11.** (a) SEM and (b) HRTEM image of A-$NiO_x$-20/$Mn_5$-$Ni_2P$ after HER stability test for 20 h in 1 M KOH.

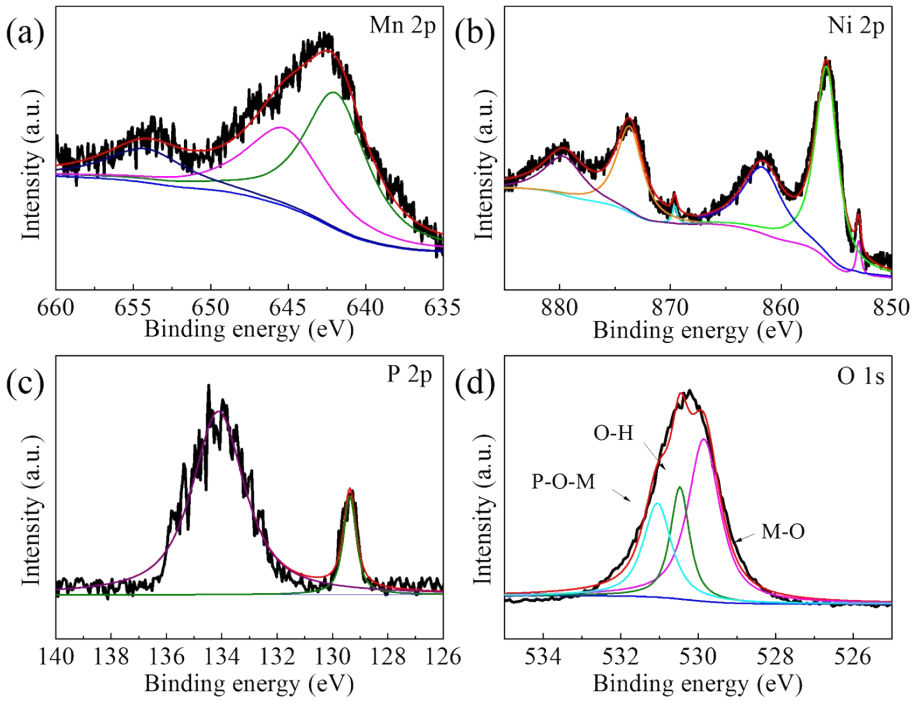


**Figure S12.** The high resolution XPS spectra of A-$NiO_x$-20/$Mn_5$-$Ni_2P$ after HER stability test for 20 h. (a) Mn 2p, (b) Ni 2p, (c) P 2p and (d) O 1s.

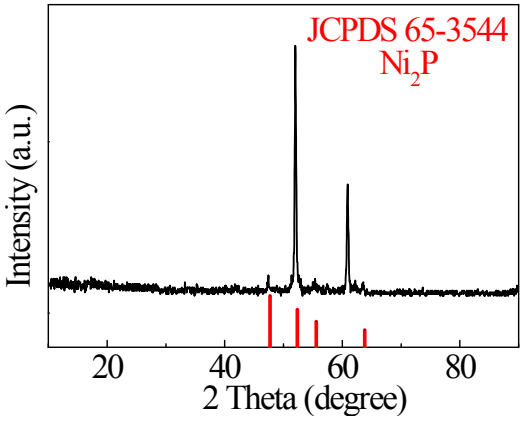


**Figure S13.** XRD pattern of A-$NiO_x$-20/$Mn_5$-$Ni_2P$ after HER stability test for 20 h in 1 M KOH.

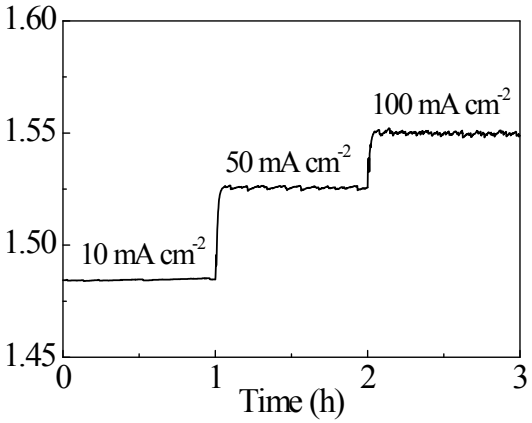


**Figure S14.** Controlled-current electrolysis of A-$NiO_x$-20/$Mn_5$-$Ni_2P$ at 10, 50 and 100 mA $cm^{-2}$ for OER.

**Table S2.** Comparison of the OER activity for several recently reported catalysts in 1 M KOH.

| Catalyst | Mass loading (mg $cm^{-2}$) | $\eta_{10}$ (mV) | Tafel (mV $dec^{-1}$) | Reference |
|---|---|---|---|---|
| A-$NiO_x$-20/$Mn_5$-$Ni_2P$ | 3.6 | 255 | 55 | This work |
| IrO2 | 2.2 | 352 | 82 | 4 |
| Fe- and O-doping CoP nanowires/NF | 2.2 | 275 | 52 | 4 |
| CoP nanosheet arrays/CC | 2.6 | 300 | 85 | 14 |
| CoNiFeP nanocubes | 0.283 | 273 | 35 | 15 |
| Fe-$CoS_2$/NF | / | 302 | 128 | 16 |
| $Ni_2P$/$(NiFe)_2P(O)$/NF | / | 150 | 60 | 17 |
| P-Co-Fe-B | 0.46 | 225 | 40 | 18 |
| $Ni_2P$ nanoparticles | 0.14 | 290 | 47 | 19 |

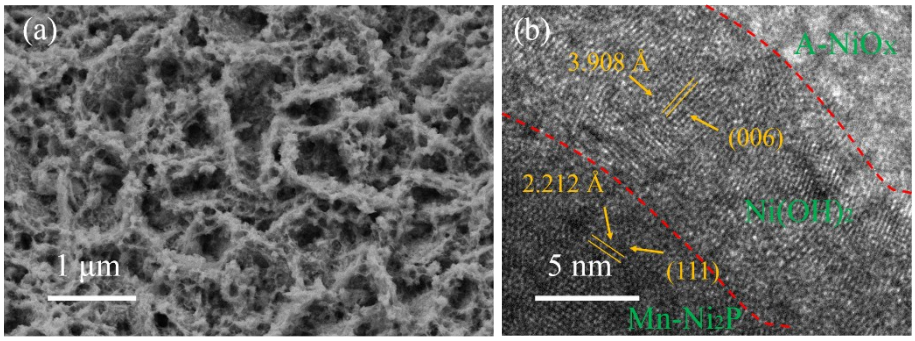


**Figure S15.** (a) SEM and (b) HRTEM image of A-$NiO_x$-20/$Mn_5$-$Ni_2P$ after OER stability test for 20 h in 1 M KOH.

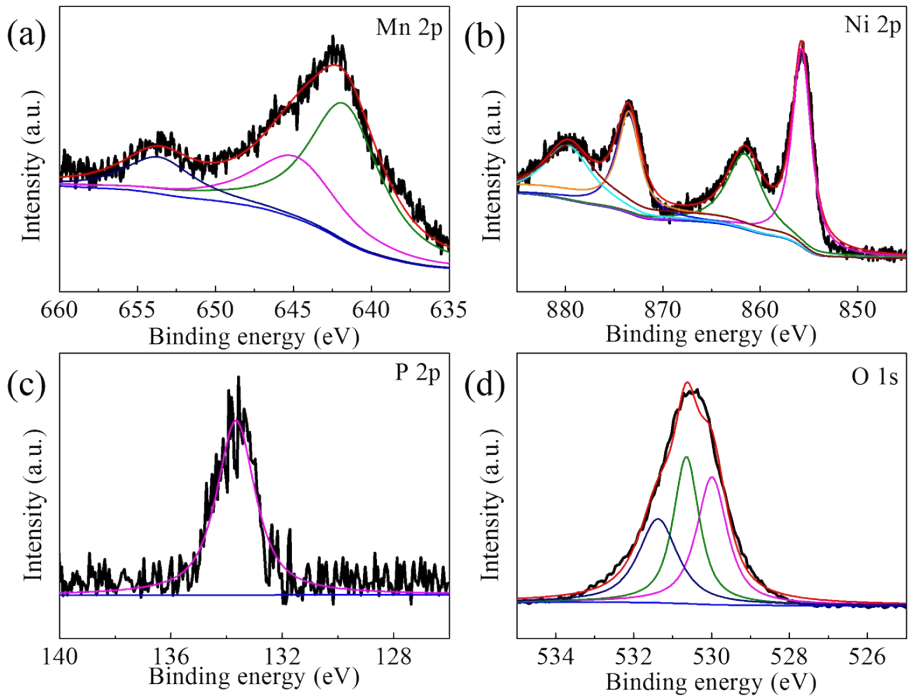


**Figure S16.** The high resolution XPS spectra of A-$NiO_x$-20/$Mn_5$-$Ni_2P$ after OER stability test for 20 h. (a) Mn 2p, (b) Ni 2p, (c) P 2p and (d) O 1s.

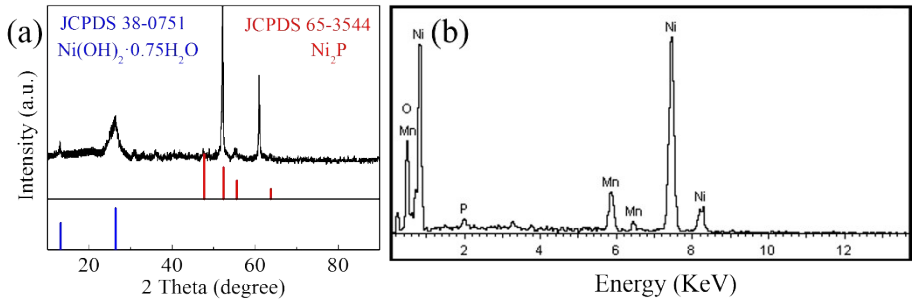


**Figure S17.** (a) XRD pattern and (b) EDS spectrum of A-$NiO_x$-20/$Mn_5$-$Ni_2P$ after OER stability test for 20 h in 1 M KOH.

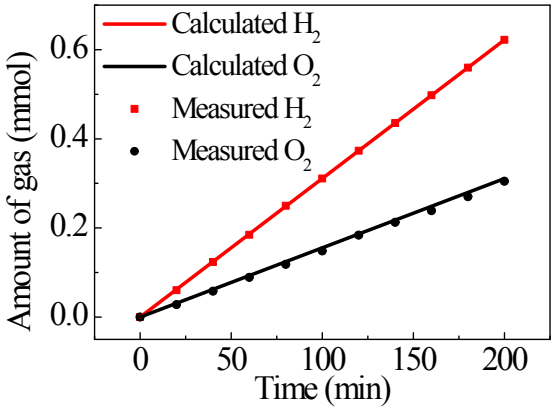


**Figure S18.** Experimentally measured and theoretically calculated amounts of $H_2$ and $O_2$ versus time for A-$NiO_x$-20/$Mn_5$-$Ni_2P$ at a fixed current density of 10 mA $cm^{-2}$.

**Notes and references**


1. G. F. Chen, T. Y. Ma, Z. Q. Liu, N. Li, Y. Z. Su, K. Davey and S. Z. Qiao, *Adv. Funct. Mater.*, 2016, **26**, 3314-3323.
2. X. Wang, W. Li, D. Xiong, D. Y. Petrovykh and L. Liu, *Adv. Funct. Mater.,* 2016, **26**, 4067-4077.
3. L. Yang, Z. Guo, J. Huang, Y. Xi, R. Gao, G. Su, W. Wang, L. Cao and B. Dong, *Adv. Mater.*, 2017, **29**, 1704574.
4. J. Duan, S. Chen, A. Vasileff and S. Z. Qiao, *ACS Nano,* 2016, **10**, 8738-8745.
5. Y. P. Zhu, Y. P. Liu, T. Z. Ren and Z. Y. Yuan, *Adv. Funct. Mater.*, 2015, **25**, 7337-7347.
6. J. Yu, Q. Li, Y. Li, G. Y. Xu, L. Zhen, V. P. Dravid and J. Wu, *Adv. Funct. Mater.*, 2016, **26**, 7644-7651.
7. P. Zhang, H. Chen, M. Wang, Y. Yang, J. Jiang, B. Zhang, L. Duan, Q. Daniel, F. Li and L. Sun, *J. Mater. Chem. A*, 2017, **5**, 7564-7570.
8. I. K. Mishra, H. Zhou, J. Sun, F. Qin, K. Dahal, J. Bao, S. Chen and Z. Ren, *Energy Environ. Sci.*, 2018, **11**, 2246-2252
9. J. Yu, Y. Zhong, X. Wu, J. Sunarso, M. Ni, W. Zhou and Z. Shao, *Adv. Sci.*, 2018, **5**, 1800514.
10. D. H. Ha, B. Han, M. Risch, L. Giordano, K. P. C. Yao, P. Karayaylali and Y. S. Horn, *Nano Energy*, 2016, **29**, 37-45.
11. C. Y. Son, I. H. Kwak, Y. R. Lim and J. Park, *Chem. Commun.*, 2016, **52**, 2819-2822.
12. X. Zhang, S. Zhang, J. Li and E. Wang, *J. Mater. Chem. A*, 2017, **5**, 22131-22136.
13. Z. Xiao, Y. Wang, Y. C. Huang, Z. Wei, C. L. Dong, J. Ma, S. Shen, Y. Li and S. Wang, *Energy Environ. Sci.*, 2017, **10**, 2563-2569.
14. T. Liu, L. Xie, J. Yang, R. Kong, G. Du, A. M. Asiri, X. Sun and L. Chen, *ChemElectroChem*, 2017, **4**, 1840-1845.
15. Y. Guo, J. Tang, Z. Wang, Y. Sugahara and Y. Yamauchi, *Small*, 2018, **14**, 1802442.
16. W. Kong, X. Luan, H. Du, L. Xia and F. Qu, *Chem. Commun.*, 2019, **55**, 2469-2472.
17. W. Xi, G. Yan, Z. Lang, Y. Ma, H. Tan, H. Zhu, Y. Wang and Y. Li, *Small*, 2018, **14**,

1802204.
18. Z. Wu, D. Nie, M. Song, T. Jiao, G. Fu and X. Liu, *Nanoscale*, 2019, **11**, 7506-7512.
19. L. A. Stern, L. Feng, F. Song and X. Hu, *Energy Environ. Sci.*, 2015, **8**, 2347-2351.
20.